IET Radar, Sonar & Navigation

Research Article

IET Journals
The Institution of Engineering and Technology

Robust wideband beamforming method for linear frequency modulation signals based on digital dechirp processing

ISSN 1751-8784
Received on 19th June 2018
Revised 13th September 2018
Accepted on 20th September 2018
E-First on 31st October 2018
doi: 10.1049/iet-rsn.2018.5267
www.ietdl.org

Weixing Li[1], *Jian Yang*[2,3] ✉, *Yue Zhang*[1], *Jian Lu*[2]

[1]*Science and Technology on Automatic Target Recognition Laboratory, National University of Defense Technology, Changsha 410073, People's Republic of China*

[2]*Rocket Force University of Engineering, Xi'an 710025, People's Republic of China*

[3]*School of Electronic Engineering, Xidian University, Xi'an 710071, People's Republic of China*

✉ *E-mail: yjep163@163.com*

Abstract: This study presents a robust digital beamforming (DBF) method for wideband digital array radar, which uses linear frequency modulation (LFM) waveforms. Firstly, received signals are digitally dechirped, followed by narrowband filtering and decimation. Then the authors generate time-variant factors to compensate phase perturbations induced by the dechirp processing. It is proved that the wideband LFM signals can be treated as narrowband signals after compensation. Finally, a robust adaptive narrowband DBF method based on uncertain set constraints and interference-plus-noise matrix reconstruction is applied to suppress the interferences. The proposed method is computationally efficient and feasible for real-time applications. It behaves robustly in the presence of direction of arrival estimation errors across a wide range of signal-to-noise ratios. Simulations demonstrate the effectiveness and feasibility of the proposed method.

1 Introduction

Wideband digital array radar (WDAR) has the potential of achieving high resolution and dynamic range. Moreover, it can be configured to different working-modes to perform different functions for various purposes, such as target detection, tracking, imaging, recognition and signal reconnaissance. In the last decade, with the development of array signal processing [1], WDAR has been widely used in radio astronomy, space surveillance and communications [2].

As one of the key technologies in array signal processing, digital beamforming (DBF) has attracted much attention [3]. An adaptive DBF approach based on genetic algorithm is proposed in [4], which is suitable for real-time control of antenna arrays. However, most previous DBF algorithms may suffer from severe performance degradation when model mismatches exist. As a result, many robust adaptive wideband DBF algorithms have been proposed to deal with the problem. Diagonal loading of the correlation matrix is a popular technique to increase the robustness of array systems [5]. However, the selection of the loading level is a crucial problem. To overcome the difficulties, a new variable loading technique, which combines the features of variable optimal loading and general linear combination, is developed in [6]. Another kind of robust beamformer is proposed in [7, 8]. It guarantees the robustness against steering vector mismatches using probability constraints. A wideband robust DBF method based on frequency invariance constraints is proposed in [9]. This method incorporates a response variation element into the robust linearly constrained minimum variance beamformer to control the consistency of the responses over the frequency range.

The requirement for high resolution results in a large bandwidth. As a result, the traditional wideband DBF algorithms suffer from high computational complexity. In addition, it may have higher requirements for transmission and storage devices owing to high data rate, which results in greater difficulty in realisation. In order to address the problems, dechirp technology [10] is widely applied in wideband radar, leading to the study of DBF algorithms based on the dechirp processing. In [11], a post-dechirp canceller is performed in both the time domain and frequency domain, which is useful to null sidelobe interferences over extremely large bandwidth. Rabideau from MIT Lincoln laboratory analysed the impact of two basic adaptive beamforming approaches on the time sidelobes of WDAR utilising dechirp processing and verified their performances using measured data [12]. However, these approaches are still based on wideband DBF architectures. A dechirp-based method is proposed in [13] which combines the wideband phase compensation weights and narrowband weights to produce the optimal weights. This method is computationally efficient, but it requires to know the directions of the interferences. To cope with the problems, several improved methods are developed, which make use of minimum variance distortionless response (MVDR) to null interferences adaptively [14, 15]. However, these methods assume that the direction of arrival (DOA) of the signal of interest (SOI) is precisely known, but the information may not be available in practice.

The aforementioned methods are based on the analogue dechirp processing. Since the reference signals are generated by analogue devices, distortions may be induced to array systems [16]. Recently, a digital dechirp technique is developed in [17], which has the same advantages as analogue dechirp but does not induce such distortions.

In this paper, we propose a digital dechirp-based DBF method for WDAR. It is shown that the digital dechirp processing will induce time-variant phase perturbations to the SOI. Hence time-variant factors are generated to compensate the perturbations. In this way, the wideband SOI can be treated as a narrowband signal. Then we prove that the steering vector of the SOI belongs to an uncertain set in the presence of direction estimation errors. Consequently, an adaptive narrowband DBF approach is applied to increase the robustness of the beamformer. The proposed method performs beamforming on wideband linear frequency modulation (LFM) signals simply by combining the time-variant compensation and the narrowband beamforming. It has much lower computational complexity than traditional wideband DBF methods.

The remaining of this paper is organised as follows. In Section 2, the signal models based on digital dechirp are demonstrated. Section 3 presents a robust adaptive DBF method applied to the dechirped signals. Simulation results are illustrated in Section 4, followed by the conclusion in Section 5.

2 Problem formulation

In a WDAR, the transmitted LFM waveform can be expressed as

$$s(t) = \cos\left[2\pi\left(f_0 t + \frac{1}{2}\mu t^2\right)\right] \cdot \mathrm{rect}\left(\frac{t}{T_0}\right) \tag{1}$$

where f_0 is the carrier frequency, μ is the chirp rate, and T_0 is the pulse width. The bandwidth is $B = \mu T_0$. $\mathrm{rect}(x) = 1$ when $-(1/2) \le x \le (1/2)$, otherwise, $\mathrm{rect}(x) = 0$.

Suppose the receiving antenna of the WDAR is an N-element wideband uniform linear array (ULA) with inter-element spacing d. Assume that the target is located at the direction of θ_s with a distance from the first element denoted by R_s. For a moving target, the Doppler effect is equivalent to a change to in time scale [18]. Unlike traditional analogue dechirp-based radar, WDAR systems usually have high-rate ADCs, which is able to sample radio-frequency echoes directly without any intermediate-frequency steps according to the band-pass sampling theory. As a result, demodulation and dechirp can be performed in the digital domain. After direct sampling and demodulating, the received signal in the kth element is

$$\begin{aligned} x_k^{(1)}(n) = \rho_s \exp[\mathrm{j}2\pi(f_0\beta(nT_\mathrm{s} - t_\mathrm{s} - \tau_k) \\ + \frac{1}{2}\mu\beta^2(nT_\mathrm{s} - t_\mathrm{s} - \tau_k)^2)\Big] \\ \cdot \mathrm{rect}\left(\frac{\beta(nT_\mathrm{s} - t_\mathrm{s} - \tau_k)}{T_0}\right) + I_k^{(1)}(nT_\mathrm{s}) \end{aligned} \tag{2}$$

where $t_\mathrm{s} = 2R_s/c$ and $\tau_k = (k-1)\, d \sin\theta_s/c$, $\beta = (c-v)/(c+v)$ is the Doppler factor. v is the relative velocity between the target and the WDAR, and c is the speed of light. ρ_s denotes the amplitude of the SOI. T_s is the sampling interval. $I_k^{(1)}(nT_s)$ contains the interferences and the noise. In this paper, the noise is assumed to be Gaussian white noise.

The basic ideal of digital dechirp [17] is mixing the received signal with a reference signal. In order to generate the reference signals, the distance and the velocity of the target must be obtained. Generally, the WDAR has multi-functions and works in multi-modes. For example, the narrowband mode is mainly used for target detection and tracking, while the wideband mode is used for imaging. The two modes are usually used alternatively. Therefore, R_s and v can be estimated by Multiple Signal Classification method in [19] when the WDAR works in the narrowband mode. Denoting the estimated distance and velocity as R_r and $\hat{v}$, the reference signal is set as [20]

$$\begin{aligned} s_\mathrm{r}(n) = \exp\left\{\mathrm{j}2\pi\left(f_0\hat{\beta}(nT_\mathrm{s} - t_\mathrm{r}) + \frac{1}{2}\mu\hat{\beta}^2(nT_\mathrm{s} - t_\mathrm{r})^2\right)\right\} \\ \cdot \mathrm{rect}\left(\frac{\hat{\beta}(nT_\mathrm{s} - t_\mathrm{r})}{T_\mathrm{r}}\right) \end{aligned} \tag{3}$$

where $t_\mathrm{r} = (2R_\mathrm{r}/c)$ and $\hat{\beta} = (c - \hat{v})/(c + \hat{v})$. T_r denotes the pulse width of the reference signal pertaining to $T_\mathrm{r} > T_0$.

Substituting (2) with (3) yields the dechirped signal

$$\begin{aligned} x_k^{(2)}(n) = \rho_s \exp\{\mathrm{j}2\pi\Big[f_0(\beta - \hat{\beta})nT_\mathrm{s} + \frac{1}{2}\mu\left(\beta^2 - \hat{\beta}^2\right)n^2T_s^2 \\ + \mu\left(\hat{\beta}^2 t_\mathrm{r} - \beta^2 t_\mathrm{s}\right)nT_\mathrm{s} + f_0 t_\Delta + \frac{1}{2}\mu\left(\beta^2 t_\mathrm{s}^2 - \hat{\beta}^2 t_\mathrm{r}^2\right)\Big]\Big\} \\ \cdot \exp\left\{\mathrm{j}2\pi\left[-\mu\beta^2\tau_k nT_\mathrm{s} - f_0\beta\tau_k + \mu\beta^2 t_\mathrm{s}\tau_k + \frac{1}{2}\mu\beta^2\tau_k^2\right]\right\} \\ \cdot \mathrm{rect}\left(\frac{\beta(nT_\mathrm{s} - t_\mathrm{s} - \tau_k)}{T_0}\right) + I_k^{(2)}(nT_\mathrm{s}) \end{aligned} \tag{4}$$

where $t_\Delta = \hat{\beta}t_\mathrm{r} - \beta t_\mathrm{s}$ and $I_k^{(2)}(nT_\mathrm{s}) = I_k^{(1)}(nT_\mathrm{s}) \cdot s_\mathrm{r}^*(nT_\mathrm{s})$.

It is noted that the SOI is approximately transformed into a tone by digital dechirp. The bandwidth of the dechirped SOI, denoted as B_dc, is mainly determined by the relative distance between t_r and t_s. If we add a narrowband filter with the bandwidth $B_\mathrm{p} \ge B_\mathrm{dc}$ after the digital dechirp processing, the SOI will not be affected by the filter. Since B_p is usually much narrower than B, a decimator can be inserted following the filter. Therefore, by applying the narrowband filter and the decimator to (4), the signal becomes

$$\begin{aligned} x_k^{(3)}(n) = \rho_s \exp\Big\{\mathrm{j}2\pi\Big[f_0\left(\beta - \hat{\beta}\right)nT_\mathrm{s}' + \frac{1}{2}\mu\left(\beta^2 - \hat{\beta}^2\right)n^2T_s'^2 \\ + \mu\left(\hat{\beta}^2 t_\mathrm{r} - \beta^2 t_\mathrm{s}\right)nT_\mathrm{s}' + f_0 t_\Delta + \frac{1}{2}\mu\left(\beta^2 t_\mathrm{s}^2 - \hat{\beta}^2 t_\mathrm{r}^2\right)\Big]\Big\} \\ \cdot \exp\left\{\mathrm{j}2\pi\left[-\mu\beta^2\tau_k nT_\mathrm{s}' - f_0\beta\tau_k + \mu\beta^2 t_\mathrm{s}\tau_k + \frac{1}{2}\mu\beta^2\tau_k^2\right]\right\} \\ \cdot \mathrm{rect}\left(\frac{\beta(nT_\mathrm{s}' - t_\mathrm{s} - \tau_k)}{T_0}\right) + I_k^{(3)}(nT_\mathrm{s}') \end{aligned} \tag{5}$$

where D denotes the decimation factor and $T_\mathrm{s}' = DT_\mathrm{s}$. $I_k^{(3)}(nDT_\mathrm{s})$ is obtained by applying the filter and decimator to $I_k^{(2)}(nT_\mathrm{s})$.

Here we denote the aforementioned steps as pre-processing, including direct sampling, demodulation, digital dechirping, narrowband filtering and decimation. It can be seen that the data rate of the pre-processed signal in (5) is decreased by a factor of D compared with that in (2). As a result, there will be a significant reduction in the requirements for the transmission and storage devices. Moreover, the interferences and noise $I_k^{(2)}(nT_\mathrm{s})$ will be filtered if their power is out of the pass-band B_p.

In [21–23], a method via a judiciously designed spatial transformation followed by a bank of highpass filters has been proposed to mitigate the effect of white noise without affecting the directional signals in wideband arbitrary linear arrays. With this method, a maximum 3 dB improvement in total power-to-total-noise-power ratio (TSNR) can be achieved in the ideal case, but the amount of calculation has been greatly increased. Compared with this method, the proposed method that performs beamforming after dechirping may greatly reduce the amount of calculation and is evidently more effective in realisation.

Due to the effects of pre-processing, the signals in (5) have different forms with traditional wideband signals. In the next section, we devote to find a DBF method which can be applied to the signals (5).

3 Robust adaptive DBF method applied to dechirped signals

3.1 Time-variant compensation

Equation (5) can be written in the form of

$$\begin{aligned} x_k^{(3)}(n) = H_\mathrm{s}(n)\exp(-\mathrm{j}2\pi f_0\beta\tau_k)g_k(n) \\ \cdot \mathrm{rect}\left(\frac{\beta(nT_\mathrm{s}' - t_\mathrm{s} - \tau_k)}{T_0}\right) + I_k^{(3)}(n) \end{aligned} \tag{6}$$

where $H_\mathrm{s}(n)$ and $g_k(n)$ are

$$\begin{cases} H_\mathrm{s}(n) = \rho_s \exp\Big\{\mathrm{j}2\pi\Big[f_0\left(\beta - \hat{\beta}\right)nT_\mathrm{s}' + \frac{1}{2}\mu\left(\beta^2 - \hat{\beta}^2\right)n^2T_\mathrm{s}'^2 \\ + \mu\left(\hat{\beta}^2 t_\mathrm{r} - \beta^2 t_\mathrm{s}\right)nT_\mathrm{s}' + f_0 t_\Delta \\ + \frac{1}{2}\mu\left(\beta^2 t_\mathrm{s}^2 - \hat{\beta}^2 t_\mathrm{r}^2\right)\Big]\Big\} \\ g_k(n) = \exp\left[\mathrm{j}2\pi\left(-\mu\beta^2 nT_\mathrm{s}'\tau_k + \mu\beta^2 t_\mathrm{s}\tau_k + \frac{1}{2}\mu\beta^2\tau_k^2\right)\right] \end{cases} \tag{7}$$

As seen from (6), $H_\mathrm{s}(n)$ is independent of τ_k and is identical for all elements. It has, therefore, no effect on DBF. The term $\exp(-\mathrm{j}2\pi f_0\beta\tau_k)$ has the same form as the steering vector of narrowband signals, which can be compensated by narrowband DBF methods. However, $g_k(n)$ is a function of τ_k and varies with the time. As a result, it is difficult to be compensated only by

narrowband weights and may deteriorate the performance of narrowband DBF algorithms seriously. Therefore, it is necessary to compensate the time-variant term in each element before applying narrowband DBF algorithms.

It is noted that the direction θ_s, the distance R_s and the velocity v, corresponding to τ_k, t_s and β, may not be known precisely. Hence it is difficult to obtain the accurate value of $g_k(n)$. Fortunately, θ_s, R_s and v can be estimated when the WDAR works in the narrowband mode. Denoting the estimation of θ_s as $\bar{\theta}_s$, the time-variant compensation factor for the kth element can be selected as

$$u_k(n) = \exp\left[\mathrm{j}2\pi\left(-\mu\beta'^2 nT_s'\bar{\tau}_k + \mu\beta'^2 t_r\bar{\tau}_k + \frac{1}{2}\mu\beta'^2\bar{\tau}_k^2\right)\right] \tag{8}$$

where $\bar{\tau}_k = (k-1)d\sin\bar{\theta}_s/c$. Here we use t_r as an estimation of t_s.

By compensating (6) with (8), we obtain

$$\begin{aligned} x_k^{(4)}(n) &= x_k^{(3)}(n)\cdot u_k^*(n) \\ &\approx H_s(n)\cdot\exp(-\mathrm{j}2\pi f_0\beta\tau_k)\exp(\mathrm{j}2\pi\Delta\phi_k(n)) \\ &\quad\cdot\mathrm{rect}\left(\frac{\beta(nT_s - t_s)}{T_0}\right) + I_k^{(4)}(n) \end{aligned} \tag{9}$$

where $I_k^{(4)}(n) = I_k^{(3)}(n)\cdot u_k^*(n)$. The residual time-variant phase is

$$\begin{aligned} \Delta\phi_k(n) &= \mu\beta^2(nT_s' - t_s)\Delta\tau_k \\ &\quad -\mu\beta^2\Delta t\bar{\tau}_k + \frac{1}{2}\mu\beta^2(\tau_k^2 - \bar{\tau}_k^2) \\ &\quad +\mu(\beta'^2 - \beta^2)\left(nT_s' - t_r - \frac{1}{2}\bar{\tau}_k\right)\bar{\tau}_k \end{aligned} \tag{10}$$

where $\Delta\tau_k = \bar{\tau}_k - \tau_k$ and $\Delta t = t_r - t_s$.

Generally, the pulse width T_0 is usually tens of microseconds, corresponding to a distance of thousands of metres. Compared with this distance, the distance estimation error $\Delta R = R_r - R_s$ and the inner-element space d are considerably small, so we have $\Delta t \ll T_0$, $\Delta\tau_k \ll T_0$.Noting that $\mu T_0 < f_0$, we can obtain $|\mu\beta^2\bar{\tau}_k\Delta t| \simeq |\mu\beta^2\tau_k\Delta t| \ll |f_0\beta\tau_k|$ and $|(1/2)\mu\beta^2(\tau_k^2 - \bar{\tau}_k^2)| \simeq |\mu\Delta\tau_k\beta^2\tau_k| \ll |f_0\beta\tau_k|$, so the second and the third terms in (10) can be ignored. In addition, the velocity v is usually much smaller than the speed of the light, leading to $\beta'^2 - \beta^2 \simeq 0$. Correspondingly, the last item can also be ignored. Therefore, the residual time-variant phase is approximately equal to

$$\Delta\phi_k(n) \simeq \mu\beta^2(nT_s' - t_s)\Delta\tau_k \tag{11}$$

Consequently, (9) can be expressed as

$$\begin{aligned} x_k^{(4)}(n) &\simeq H_s(n)\cdot\exp\left[-\mathrm{j}2\pi f_0\beta\left(\tau_k - \frac{\Delta\phi_k(n)}{\beta f_0}\right)\right] \\ &\quad\cdot\mathrm{rect}\left(\frac{\beta(nT_s' - t_s)}{T_0}\right) + I_k^{(4)}(n) \end{aligned} \tag{12}$$

In (12), we have $|(\Delta\phi_k(n)/(\beta f_0))| = |(\mu\beta(nT_s' - t_s)\Delta\tau_k/(f_0))| < \Delta\tau_k$. Therefore, the perturbation on τ_k mainly depends on $\Delta\tau_k$, which is usually very small. As a result, the SOI after time-variant compensation can be treated as a narrowband signal with a small perturbation on the time delay. Subsequently, it is possible to apply narrowband DBF algorithms.

3.2 Robust adaptive narrowband DBF algorithm

According to (12), the signals after time-variant compensation can be written in the vector form as

$$\boldsymbol{x}(n) = H_s(n)\mathrm{rect}\left(\frac{\beta(nT_s' - t_s)}{T_0}\right)\cdot\boldsymbol{a}_s + \boldsymbol{I}(n) \tag{13}$$

where

$$\begin{cases} \boldsymbol{x}(n) = \left[x_1^{(4)}(n), x_2^{(4)}(n), \ldots, x_N^{(4)}(n)\right]^{\mathrm{T}} \\ \boldsymbol{I}(n) = \left[I_1^{(4)}(n), I_2^{(4)}(n), \ldots, I_N^{(4)}(n)\right]^{\mathrm{T}} \end{cases} \tag{14}$$

$\boldsymbol{a}_s \in \mathbb{C}^{N\times 1}$ denotes the actual steering vector of the SOI defined as

$$\begin{aligned} \boldsymbol{a}_s = \Bigg[&\exp\left\{-\mathrm{j}2\pi f_0\beta\left(\tau_1 - \frac{\Delta\phi_1(n)}{\beta f_0}\right)\right\}, \\ &\exp\left\{-\mathrm{j}2\pi f_0\beta\left(\tau_2 - \frac{\Delta\phi_2(n)}{\beta f_0}\right)\right\}, \ldots, \\ &\exp\left\{-\mathrm{j}2\pi f_0\beta\left(\tau_N - \frac{\Delta\phi_N(n)}{\beta f_0}\right)\right\}\Bigg]^{\mathrm{T}} \end{aligned} \tag{15}$$

The presumed steering vector is $\bar{\boldsymbol{a}}_s = \left[\exp\left(-\mathrm{j}2\pi f_0\hat{\beta}\bar{\tau}_1\right), \exp\left(-\mathrm{j}2\pi f_0\hat{\beta}\bar{\tau}_2\right), \ldots, \exp\left(-\mathrm{j}2\pi f_0\hat{\beta}\bar{\tau}_N\right)\right]^{\mathrm{T}}$. Therefore, the mismatch between the actual steering vector and the presumed one can be obtained as

$$\boldsymbol{a}_e = \boldsymbol{a}_s - \bar{\boldsymbol{a}}_s \tag{16}$$

Considering that $-(T_0/2) \le nT_s' - t_s \le (T_0/2)$, for $k = 1, 2, \ldots, N$, we have

$$\begin{aligned} |\boldsymbol{a}_e(k)|^2 &\simeq \left|\exp(-\mathrm{j}2\pi f_0\bar{\tau}_k)\right. \\ &\quad\left.\cdot\left\{\exp\left[\mathrm{j}2\pi\left(f_0\beta + \mu\beta^2(nT_s' - t_s)\right)\Delta\tau_k\right] - 1\right\}\right|^2 \\ &\le \max\left\{2 - 2\cos\left[2\pi\left(f_0\beta + \frac{1}{2}\mu\beta^2 T_0\right)\Delta\tau_k\right],\right. \\ &\quad\left. 2 - 2\cos\left[2\pi\left(f_0\beta - \frac{1}{2}\mu\beta^2 T_0\right)\Delta\tau_k\right]\right\} \triangleq \varepsilon_k \end{aligned} \tag{17}$$

Given the bound of estimation errors of θ_s, we can obtain the bound of $\Delta\tau_k$. Subsequently, ε_k can be calculated according to (17). Therefore, the actual steering vector $\boldsymbol{a}_s$ belongs to the following uncertainty set

$$\Omega \triangleq \left\{\boldsymbol{a}_s \middle|\, \|\boldsymbol{a}_s - \bar{\boldsymbol{a}}_s\|_{\mathrm{F}}^2 \le \varepsilon_0\right\} \tag{18}$$

where $\varepsilon_0 = \sum_{k=1}^{N}\varepsilon_k$. $\|\cdot\|_{\mathrm{F}}$ denotes the Frobenius norm.

As can be seen from (13) and (18), the SOI has the same form of a narrowband signal, except that the actual steering vector belongs to the uncertainty set Ω. Based on the sample matrix inversion algorithm in [24] and the WCPO algorithm in [25], the formulation of adaptive beamformer can be written as the following constrained minimisation problem:

$$\begin{aligned} &\min_{\boldsymbol{w}} \boldsymbol{w}^{\mathrm{H}}\boldsymbol{R}_x\boldsymbol{w} \\ &\mathrm{s.t.}\ \left|\boldsymbol{w}^{\mathrm{H}}\boldsymbol{a}_s\right| \ge 1, \mathrm{for}\|\boldsymbol{a}_s - \bar{\boldsymbol{a}}_s\|^2 \le \varepsilon_0 \end{aligned} \tag{19}$$

where $\boldsymbol{R}_x = (1/K)\sum_{n=1}^{K}\boldsymbol{x}(n)\boldsymbol{x}^{\mathrm{H}}(n)$. K denotes the number of snapshots.

The beamformer in (19) is, in essence, the minimum power distortionless response (MPDR) beamformer, since $\boldsymbol{R}_x$ is calculated using the training samples which contain the SOI. However, it is well known that the MPDR beamformer is sensitive to steering vector mismatches, which are inevitable whenever DOA estimation errors exist. Moreover, the performance of the beamformer will degrade seriously at high signal-to-noise ratios (SNRs) owing to the fact that the SOI is present at the training samples. In order to improve the robustness, we reconstruct the interference-plus-noise covariance (INC) matrix.

Suppose the angle sector in which the SOI is located is $\Theta = [\theta_L, \theta_H]$. The width of Θ is determined by the DOA estimation resolution of the array system. The main requirement is that the

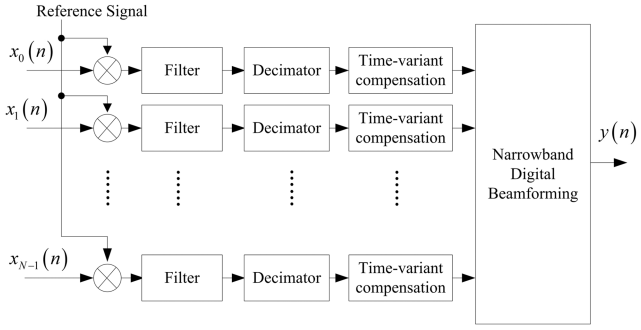

Fig. 1 *Block diagram of the proposed algorithm*

SOI is located in Θ while the interferences are not. The INC matrix can be reconstructed as [26, 27]

$$\boldsymbol{R}_{i+n} = \int_{\bar{\Theta}} \frac{\boldsymbol{b}(\theta)\boldsymbol{b}^{\mathrm{H}}(\theta)}{\boldsymbol{b}^{\mathrm{H}}(\theta)\boldsymbol{R}_x^{-1}\boldsymbol{b}(\theta)}\mathrm{d}\theta \tag{20}$$

where

$\boldsymbol{b}(\theta) = [1, \exp(-\mathrm{j}2\pi f_0 \beta d \sin\theta/c), \ldots, \exp(-\mathrm{j}2\pi f_0 \beta (N-1) d \sin\theta/c)]^{\mathrm{T}}$

$\bar{\Theta} = [-90°, \theta_{\mathrm{L}}] \cup [\theta_{\mathrm{H}}, 90°]$ is the complimentary sector of Θ.

By replacing $\boldsymbol{R}_x$ with $\boldsymbol{R}_{i+n}$, the problem in (19) becomes

$$\begin{aligned} &\min_{\boldsymbol{w}} \boldsymbol{w}^{\mathrm{H}}\boldsymbol{R}_{i+n}\boldsymbol{w} \\ &\text{s.t. } \left|\boldsymbol{w}^{\mathrm{H}}\boldsymbol{a}_{\mathrm{s}}\right| \geq 1, \quad \text{for } \| \boldsymbol{a}_{\mathrm{s}} - \bar{\boldsymbol{a}}_{\mathrm{s}} \|^2 \leq \varepsilon_0 \end{aligned} \tag{21}$$

The problem in (21) belongs to the category of adaptive DBF algorithm constrained by an uncertain set. As a result, it is capable to obtain the solution using the method in [28] as follows:

$$\boldsymbol{w} = \frac{(\boldsymbol{R}_{i+n} + \lambda \boldsymbol{I})^{-1}\bar{\boldsymbol{a}}_{\mathrm{s}}}{\bar{\boldsymbol{a}}_{\mathrm{s}}^{\mathrm{H}}(\boldsymbol{R}_{i+n} + \lambda \boldsymbol{I})^{-1}\boldsymbol{R}_{i+n}(\boldsymbol{R}_{i+n} + \lambda \boldsymbol{I})^{-1}\bar{\boldsymbol{a}}_{\mathrm{s}}} \tag{22}$$

where λ is the diagonal loading factor, which can be calculated by Newton's method.

Finally, the output of the beamformer can be obtained by applying the narrowband weights $\boldsymbol{w}$ to (13)

$$y(n = \boldsymbol{w}^{\mathrm{H}}\boldsymbol{x}(n) \tag{23}$$

In summary, the proposed method is carried out by three steps: pre-processing, time-variant compensation followed by narrowband beamforming, as shown in Fig. 1. It is worth mentioning that the data rate is decreased by a factor of D after pre-processing. It is effective to reduce the burdens of computation, transmission and storage in the subsequent processing. Moreover, the proposed method only calculates the narrowband weights at f_0, instead of those at a set of frequency bins. Therefore, the proposed method has a much lower computational complexity compared with traditional wideband DBF algorithms.

4 Numerical assessment

In this section, several representative simulations are carried out to demonstrate the performance of the proposed method.

Consider a wideband monopole antenna array with $N = 16$ elements arranged uniformly on a line. The operation frequency is [2.45, 2.95 GHz]. With the purpose of avoiding grating lobes, the distance between neighbouring elements is set as $d = 0.05$ m, which is about the half wavelength of the highest frequency. The signals are directly sampled by an analogue-to-digital converter (ADC) at a rate of 1.2 Gsps.

In the first simulation, the transmitted signal is modeled as an LFM signal with the bandwidth of $B = 400$ MHz at a center frequency of 2.7 GHz. The pulse width is $T_0 = 25$ μs and the range window is set as $\Delta R_{\max} = 100$m. The target is located at 20 m away from the reference distance at the direction of −15°. The presumed direction is −16° with the estimation error as 1°. The target moves with a velocity of $v_0 = 5000$ m/s with respect to the radar, while the estimation of the velocity is $\tilde{v} = 4900$ m/s. There are two interferences with the same frequency band impinging on the array from 10° and 35°, respectively. Without loss of generality, the interferences have arbitrary waveforms, which are produced using the 'randn' function in MATLAB followed by band-pass filters. The SNR is set as −5 dB and the INR is set as 20 and 20 dB.

It is noted that the complex sampling rate after demodulation is 600 Msps. Suppose the output bit width is 16bits, the data rate of the received signal is 600 Msps*16 bits = 9.6 Gbps, which is relatively high for transmitting. Considering the bandwidth of the dechirped SOI is limited to $B_{\mathrm{dc}} = (B/T_0) \cdot (2\Delta R_{\max}/c) = 10.66$ MHz, the pass-band of the narrowband filter is set as $B_{\mathrm{p}} = 12$ MHz, followed by a decimator with a factor of $D = 32$. Therefore, after the decimation, the data rate is only 9.6 Gsps/32 = 300 Mbps, which is reduced significantly. Moreover, the interferences which spread their spectrums out of B_{p} are filtered, as shown in Fig. 2*a*. However, the SOI is still not available since the interferences within B_{p} are preserved by the bandpass filter. Fig. 2*b* shows the beam pattern. The pulse compression of the output signal is shown in Fig. 2*c*. The spectrum of the interferences is suppressed to lower than 10 dB, and subsequently, the peak of the SOI can be recognised.

Fig. 3 shows the output SINR versus different SNR varying from −10 to 20 dB. We run 200 Monte Carlo trials for each condition in the simulations unless specially mentioned. In comparison, we also illustrate the results of the previous dechirp-based DBF method in [14], the wideband robust frequency invariant worst-case (RB-FI-WC) DBF method in [9]. The optimal SINR is also given for comparison, which is obtained in ideal conditions. In [14], the diagonal loading level is set as 10 dB with respect to the white noise level, and the notch width is set as 0.05. In [9], the number of delay-taps is set as 20, and the MATLAB tool box 'CVX' is used to find the solutions of optimal problems. In the proposed method, the angle sector of the SOI is set as $\Theta = [-20°, -10°]$. As seen from the figure, the performance of the proposed method is close to the optimal SINR over a large range from −10 to 20 dB. However, the performance of the method in [14] is deteriorated seriously at high SNR due to the effects of the SOI. The method in [9] also suffers from performance degradation at high SNR.

Setting the SNR as 5 dB while keeping other conditions unchanged, we run each of the three methods for 200 times. All the simulations are taken by the MATLAB R2014a platform on a computer with Inter Core i5–2320 CPU. The time cost of each method is illustrated in Table 1. As seen from the table, the total time cost of the three methods is 6369.0, 136.1, 157.5 s, respectively. The method in [9] is very time-consuming because it deals with the wideband signals using the CVX tools. In comparison, the other two methods, which conduct DBF after dechirp, are much more computationally efficient and may be more suitable candidates for real-time applications. It is noted that the proposed method requires slightly more time than that of the method in [14] due to the reconstruction of the INC matrix.

We investigate the robustness of the proposed method in terms of the output SINR versus the DOA estimation errors, as illustrated in Fig. 4. Obviously, the method in [14] suffers from serious performance degradation with large DOA estimation errors, while both the proposed method and the method in [9] behave robustly. Our method is more effective in coping with the DOA estimation errors since it reaches a higher SINR.

The effects of the velocity estimation errors are shown in Fig. 5, where the SNR and the DOA estimation error are set as 5 dB and 1°. As we can see, with the increase of the velocity estimation errors, the output SINR of the three methods almost maintains the same. That means the output SINRs of these DBF methods are not sensitive to velocity estimation errors.

The interferences in the first simulation have random waveforms which spread their power throughout the whole band after dechirp. In the second simulation, we are concerned about

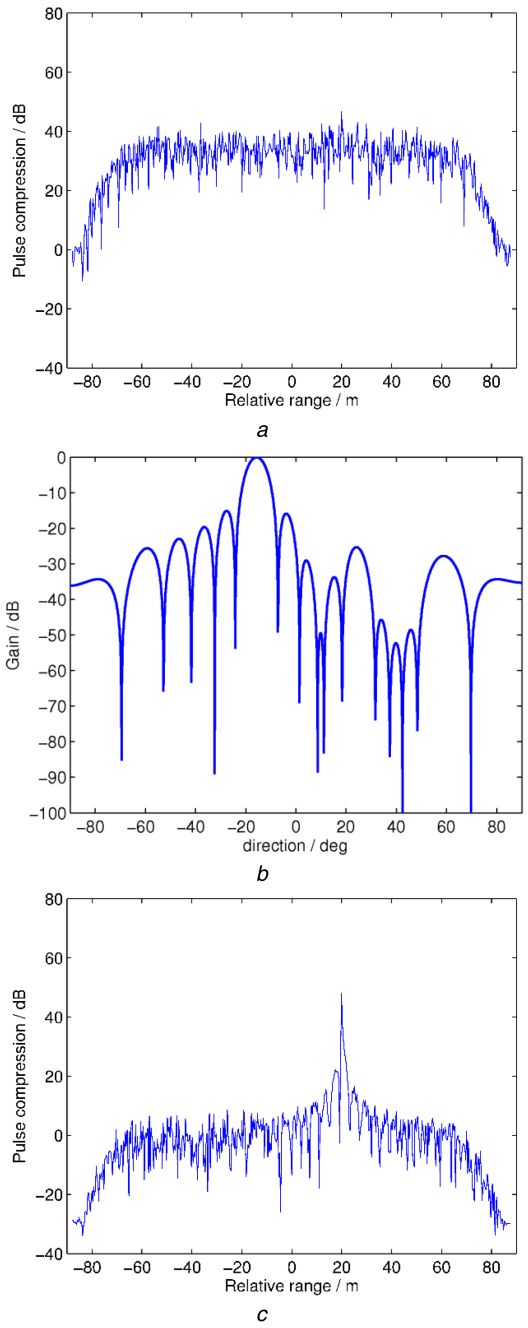

Fig. 2 *Pulse compression results*
(a) Signal in the first element after pre-processing, ***(b)*** Beam pattern, ***(c)*** Output of the beamformer

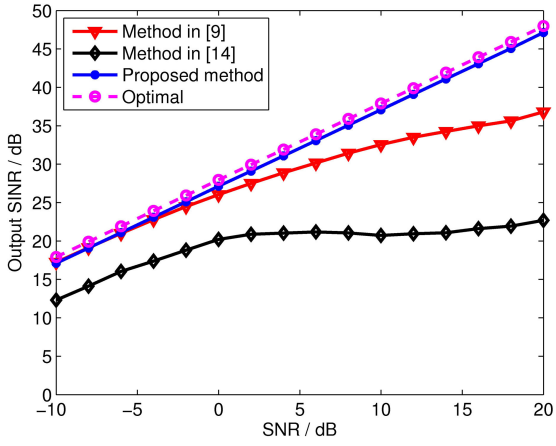

Fig. 3 *Output SINR versus input SNR with the DOA estimation error of* 1°

Table 1 Time cost of 200 Monte-Carlo runs

Methods	Method in [9]	Method in [14]	Proposed method
time cost, s	6369.0	136.1	157.5

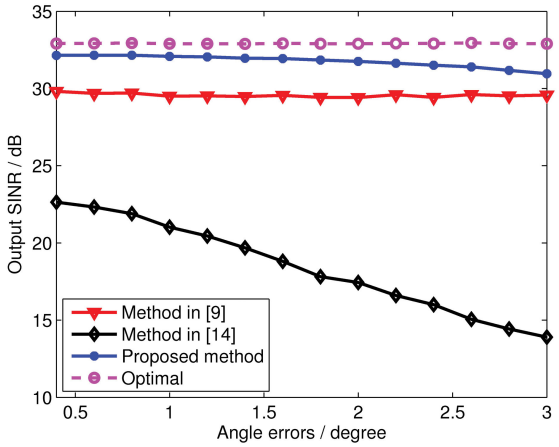

Fig. 4 *Output SINR versus DOA estimation errors with an SNR of 5 dB*

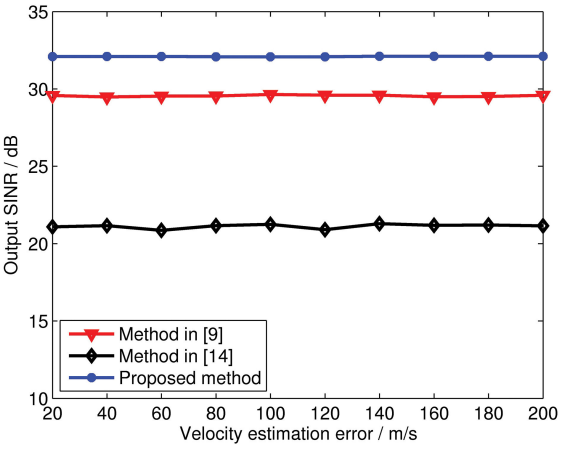

Fig. 5 *Output SINR versus velocity estimation errors with an SNR of 5 dB and the DOA estimation error of* 1°

some special cases such as active interferences. Under these situations, the power of the dechirped interferences distributes within the pass-band of the narrowband filter.

The setups are kept the same as the first simulation except that the interferences have the same LFM waveform as the SOI. The two interferences are located at −30 and 40 m away from the reference distance, respectively. The pulse compression results are shown in Fig. 6. As we can see, the peak of the SOI, located at 20 m, is about 49 dB. However, the peaks of the interferences, located at −30 and 40 m, is about 70 dB. As a result, the interferences may be mistaken as the target. Fig. 6*b* shows the beam pattern of the proposed algorithm, the gain at the directions of the interferences is 60 dB lower than that at the direction of the SOI. In Fig. 6*c*, the interferences are suppressed to about 10 dB by the beamformer, while the SOI is preserved as before.

The statistic performance of the proposed method is evaluated in the presence of the LFM interferences. The output SINR versus input SNR and DOA estimation errors are depicted in Figs. 7 and 8, respectively. The proposed method reaches a higher SINR than other methods under the same condition. The results show that the proposed method has a good performance on suppressing the interferences with the same waveform as the SOI.

5 Conclusion

An adaptive DBF method for WDAR is proposed based on the digital dechirp processing. By employing time-variant compensation factors, the wideband LFM signals are transformed

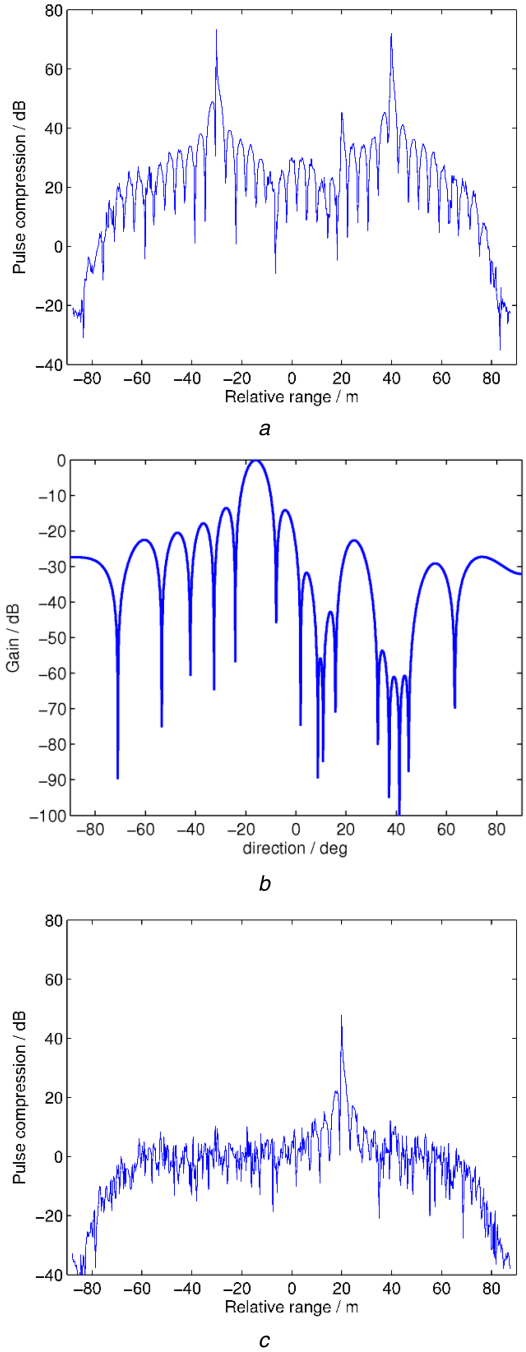

Fig. 6 *Pulse compression results in the presence of LFM interferences*
(a) Signal in the first element after pre-processing, ***(b)*** Beam pattern, ***(c)*** Output of the beamformer

into narrowband signals with small perturbations on the steering vector. Subsequently, a narrowband DBF method that combines uncertain set constraints and INC matrix reconstruction approaches are applied. The proposed method behaves robustly in the presence of the DOA and distance estimation errors. It is computationally efficient and a good candidate for real-time applications. The effectiveness of the proposed method is verified by simulations.

6 Acknowledgments

This work was supported by the National Natural Science Foundation of China under grants nos. 61501471 and 61571449.

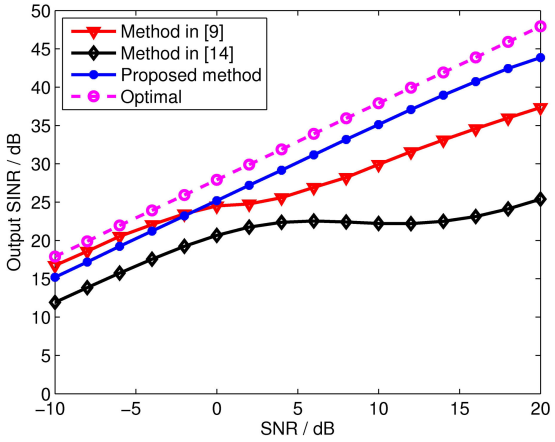

Fig. 7 *Output SINR versus input SNR in the presence of LFM interferences with the DOA estimation error of* 1°

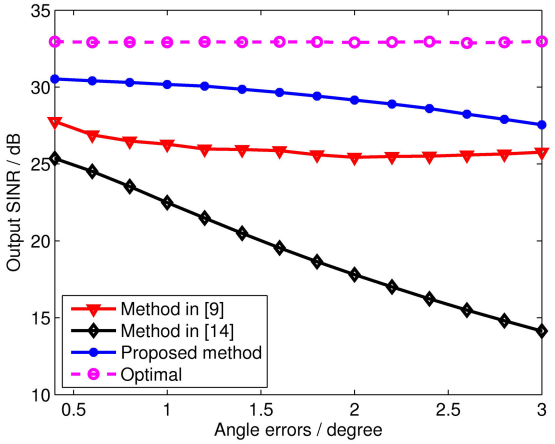

Fig. 8 *Output SINR versus DOA estimation errors in the presence of LFM interferences with an SNR of 5 dB*

7 References

[1] Donelli, M., Viani, F., Rocca, P., *et al.*: 'An innovative multiresolution approach for DOA estimation based on a support vector classification', *IEEE Trans. Antennas Propag.*, 2009, **57**, (8), pp. 2270–2292
[2] Cantrell, B., de Graaf, J., Willwerth, F., *et al.*: 'Development of a digital array radar (DAR)', *IEEE Aerosp. Electron. Syst. Mag.*, 2002, **17**, (3), pp. 22–27
[3] Liu, W, Weiss, S.: '*Wideband beamforming: concepts and techniques*' (Wiley, Chichester, UK, 2010)
[4] Massa, A., Donelli, M., De Natale, F.G.B., *et al.*: 'Planar antenna array control with genetic algorithms and adaptive array theory', *IEEE Trans. Antennas Propag.*, 2004, **52**, (11), pp. 2919–2924
[5] Carlson, B.D.: 'Covariance matrix estimation errors and diagonal loading in adaptive arrays', *IEEE Trans. Aerosp. Electron. Syst.*, 1988, **24**, pp. 397–401
[6] Hossain, M.S., Milford, G.N., Reed, M.C., *et al.*: 'Efficient robust broadband antenna array processor in the presence of look direction errors', *IEEE Trans. Antennas Propag.*, 2013, **61**, (2), pp. 718–727
[7] Vorobyov, S.A., Rong, Y., Gershman, A.B.: 'On the relationship between robust minimum variance beamformers with probabilistic and worst-case distortionless response constraints', *IEEE Trans. Signal Process.*, 2008, **56**, (11), pp. 5719–5725
[8] Liu, C.C, Liu, Y.Q., Zhao, Y.J., *et al.*: 'Robust adaptive wideband beamforming using probability-constrained optimization', *Progr. Electromagn. Res C*, 2014, **52**, pp. 163–172
[9] Zhao, Y., Liu, W., Langley, R.J.: 'Adaptive wideband beamforming with frequency invariance constraints', *IEEE Trans. Antennas Propag.*, 2011, **59**, (4), pp. 1175–1184
[10] Caputi, W.J.: 'Stretch: a time-transformation technique', *IEEE Trans. Aerosp. Electron. Syst.*, 1971, **AES-7**, (2), pp. 269–278
[11] Torres, J.A., Davis, R.M., Kramer, J.D.R., *et al.*: 'Efficient wideband jammer nulling when using stretch processing', *IEEE Trans. Aerosp. Electron. Syst.*, 2000, **36**, (4), pp. 1167–1178
[12] Rabideau, D.J., Parker, P.: 'Wideband adaptive beamforming to control time sidelobes and null depth'. Proc. of SPIE-Int. Society for Optics and Photonics, April 2003, pp. 187–199
[13] Cao, Y.H., Zhang, S.H., Luo, Y.J., *et al.*: 'Beamforming techniques of wideband and large scan angle based on stretch processing', *J. Xi'An JiaoTong Univ.*, 2004, **38**, (8), pp. 847–850
[14] Li, H.Y., Zhang, X.H., He, Z.S., *et al.*: 'A wideband digital beamforming method based on stretch processing', *WSEAS Trans. Signal Process.*, 2009, **5**, (7), pp. 251–260

[15] Luo, Y.J., Zhang, X., Cao, Y.H., *et al.*: 'Received interference nulling for wideband phased array in the presence of large scan angle', *Chin. J. Radio Sci.*, 2005, **20**, (1), pp. 43–47
[16] Lin, Q.Q., Chen, Z.P., Zhang, Y., *et al.*: 'Coherent phase compensation method based on direct IF sampling in wideband radar', *Prog. Electromagn. Res.*, 2013, **136**, pp. 753–764
[17] Lin, Q.Q., Zhang, Y., Tang, P.F., *et al.*: 'Digital de-chirp method based on wideband radar direct IF sampling', *J. Astronaut.*, 2013, **34**, (3), pp. 402–409
[18] Zhou, W., Yeh, C.M., Jin, K., *et al.*: 'ISAR imaging based on the wideband hyperbolic frequency-modulation waveform', *Sensors*, 2015, **15**, pp. 23188–23204
[19] Schemidt, R.: 'Multiple emitter location and signal parameter estimation', *IEEE Trans. Antennas Propag.*, 1986, **3**, pp. 276–280
[20] Eshbaugh, J.V., Morrison, R.L.Jr., Weber, E., *et al.*: 'HUSIR signal processing', *LINCOLN Lab. J.*, 2014, **21**, (1), pp. 115–134
[21] Anbiyaei, M.R., Liu, W., McLernon, D.C.: 'Performance improvement for wideband DOA estimation with white noise reduction based on uniform linear arrays'. Proc. IEEE, Sensor Array and Multichannel Signal Processing Workshop (SAM), Rio de Janeiro, Brazil, July 2016, pp. 1–5
[22] Anbiyaei, M.R., Liu, W., McLernon, D.C.: 'White noise reduction for wideband beamforming based on uniform rectangular arrays'. Proc. 22nd Int. Conf. on Digital Signal Processing (DSP), London, UK, November 2017, pp. 1–5
[23] Anbiyaei, M.R., Liu, W., McLernon, D.C.: 'White noise reduction for wideband linear array signal processing'. *IET Signal Processing*, 2018, **12**, (3), pp. 335–345
[24] Ehrenberg, L., Gannot, S., Leshem, A., *et al.*: 'Sensitivity analysis of MVDR and MPDR beamformers'. IEEE 26th Convention of Electrical and Electronics Engineers, Eliat, Israel, 2010, pp. 416–420
[25] Vorobyov, S.: ' robust adaptive beamforming using worst-case performance optimization: a solution to the signal mismatch problem', *IEEE Trans. Signal Process.*, 2003, **2**, pp. 313–324
[26] Gu, Y.J., Leshem, A.: 'Robust adaptive beamforming based on interference covariance matrix reconstruction and steering vector estimation', *IEEE Trans. Signal Process.*, 2012, **60**, (7), pp. 3881–3885
[27] Yang, K., Zhao, Z.Q., Liu, Q.H.: 'Robust adaptive beamforming against array calibration errors', *Progr. Electromagn. Res.*, 2013, **140**, pp. 341–351
[28] Li, J., Stoica, P., Wang, Z.S.: 'On robust capon beamforming and diagonal loading', *IEEE Trans. Signal Process.*, 2003, **51**, (7), pp. 1702–1715